J|A|C|S
ARTICLES
Published on Web 10/01/2002

Reaction Mechanism of the HGXPRTase from *Plasmodium falciparum*: A Hybrid Potential Quantum Mechanical/Molecular Mechanical Study

Aline Thomas and Martin J. Field*

Contribution from the Laboratoire de Dynamique Moléculaire Institut de Biologie Structurale Jean-Pierre Ebel, 41, rue Jules Horowitz, F-38027 Grenoble Cedex 01, France

Received May 13, 2002

Abstract: Parasites lack the ability to synthesize purines *de novo*. Instead, they use an enzyme, hypoxanthine-guanine-xanthine phosphoribosyltransferase (HGXPRTase), to salvage host purine and to construct their own nucleotides. In this paper, we investigate the reaction mechanism of the HGXPRTase from *Plasmodium falciparum* using free-energy simulations and a hybrid potential QM/MM description of the enzyme. The possibility of both dissociative and associative nucleophilic substitutions is discussed, as contradictory hypotheses have been postulated on the basis of crystallographic data and kinetic isotope effect experiments. The preferred pathway is predicted to be stepwise with a rapid proton transfer from the hypoxanthine to the protein followed by a rate-limiting glycosyl transfer. This latter step has a D_NA_N mechanism with a transition state in which the pyrophosphate leaving group is more closely bound than the attacking hypoxanthine nucleophile. The energy barrier is comparable to the experimentally observed one.

1. Introduction

Parasitic protozoa have been the subject of intense research as they are responsible for many human diseases, including malaria, giardiasis, trypanosomiasis, and toxoplasmosis. The most important of these diseases is malaria, which causes more than one million deaths each year in Africa alone, many of them children. Finding drugs to combat these organisms, however, is problematic because they are eukaryotes and so have a molecular biology that is more similar to our own than, for example, bacteria.

A potentially promising target for inhibition which could lead to chemotherapeutic compounds is the parasitic enzyme hypoxanthine-guanine-xanthine phosphoribosyltransferase (HGXPRTase). Parasitic protozoa cannot synthesize purine nucleotides *de novo*. Instead, they rely on purine phosphoribosyltransferases (PRTases) that catalyze the recovery of their hosts' purine bases and their conversion into the corresponding nucleotides (see refs 1 and 2 for reviews). In *Plasmodium falciparum*, the causative agent of malaria, the HGXPRTase salvages hypoxanthine, guanine, and xanthine and converts them into their monophosphate nucleotides, IMP (inosine monophosphate), GMP (guanosine monophosphate), and XMP (xanthosine monophosphate), respectively. These are formed by the transfer of the 5-phosphoribosyl group from the α-D-5-phosphoribosyl-1-pyrophosphate (PRPP) to a nitrogen atom of the imidazole ring of a purine base. The overall reaction that is catalyzed is shown in Figure 1.

Even though mammals can produce purine nucleotides, they also make use of purine salvage pathways and so possess PRTases. In humans, for example, there is a hypoxanthine-guanine phosphoribosyltransferase (HGPRTase) which, if absent, causes gout and the Lesch−Nyhan syndrome that leads to severe neural disorders.[3] In contrast to the case of the protozoal enzyme, the human enzyme shows a much reduced affinity for xanthine, a difference which could be crucial for the design of selective inhibitors. This aspect of the selectivity has already been investigated with molecular dynamic (MD) simulations by Pitera and co-workers.[4]

Experiments have shown that the enzyme follows an ordered reaction sequence, binding PRPP and then the purine base and releasing PPi (pyrophosphate) and then the nucleotide. The enzyme-catalyzed reaction of hypoxanthine with PRPP to give IMP and PPi occurs rapidly at pH 7.4 with forward and reverse rate constants of 131 and 9 s^{-1}, respectively, corresponding to energy barriers of about 63 and 69 kJ mol^{-1}.[5] Two of the possible mechanisms that have been hypothesized for the reaction are illustrated in Figure 2. There is a dissociative, S_N1-like mechanism that first produces PPi and a charged ribooxocarbonium ion and only afterward the nucleotide, and there is an associative, S_N2-like mechanism in which attack of the PRPP

* Telephone: (33)-4-38-78-95-94. Fax: (33)-4-38-78-54-94. E-mail: thomas@ibs.fr and mjfield@ibs.fr.

(1) Musik, Wm D. L. *Crit. Rev. Biochem.* **1981**, *X*, 1−34.
(2) Craig, S. P., III; Eakin, A. E. *J. Biol. Chem.* **2000**, *275*, 20231−34.
(3) Lesh, M.; Nyhan, W. L. *Am. J. Med.* **1964**, *36*, 561−70.
(4) Pitera, J. W.; Munagala, N. R.; Wang, C. C.; Kollman, P. A. *Biochemistry* **1999**, *38*, 10298−306.
(5) Xu, Y.; Eads, J.; Sacchettini, J. C.; Grubmeyer, C. *Biochemistry* **1997**, *36*, 3700−12.

10.1021/ja0206846 CCC: $22.00

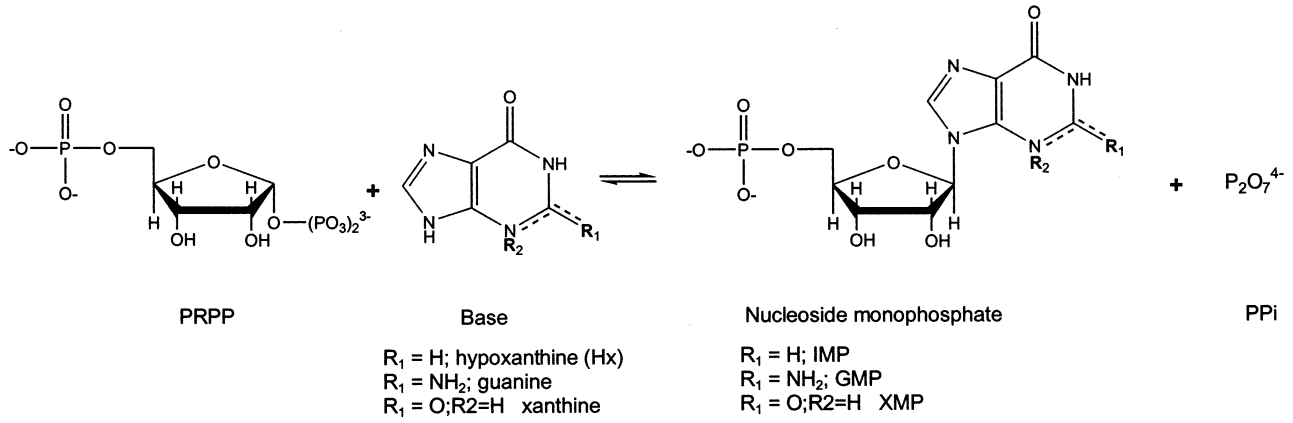

Figure 1. Schematic diagram of the reaction catalyzed by HGXPRTases

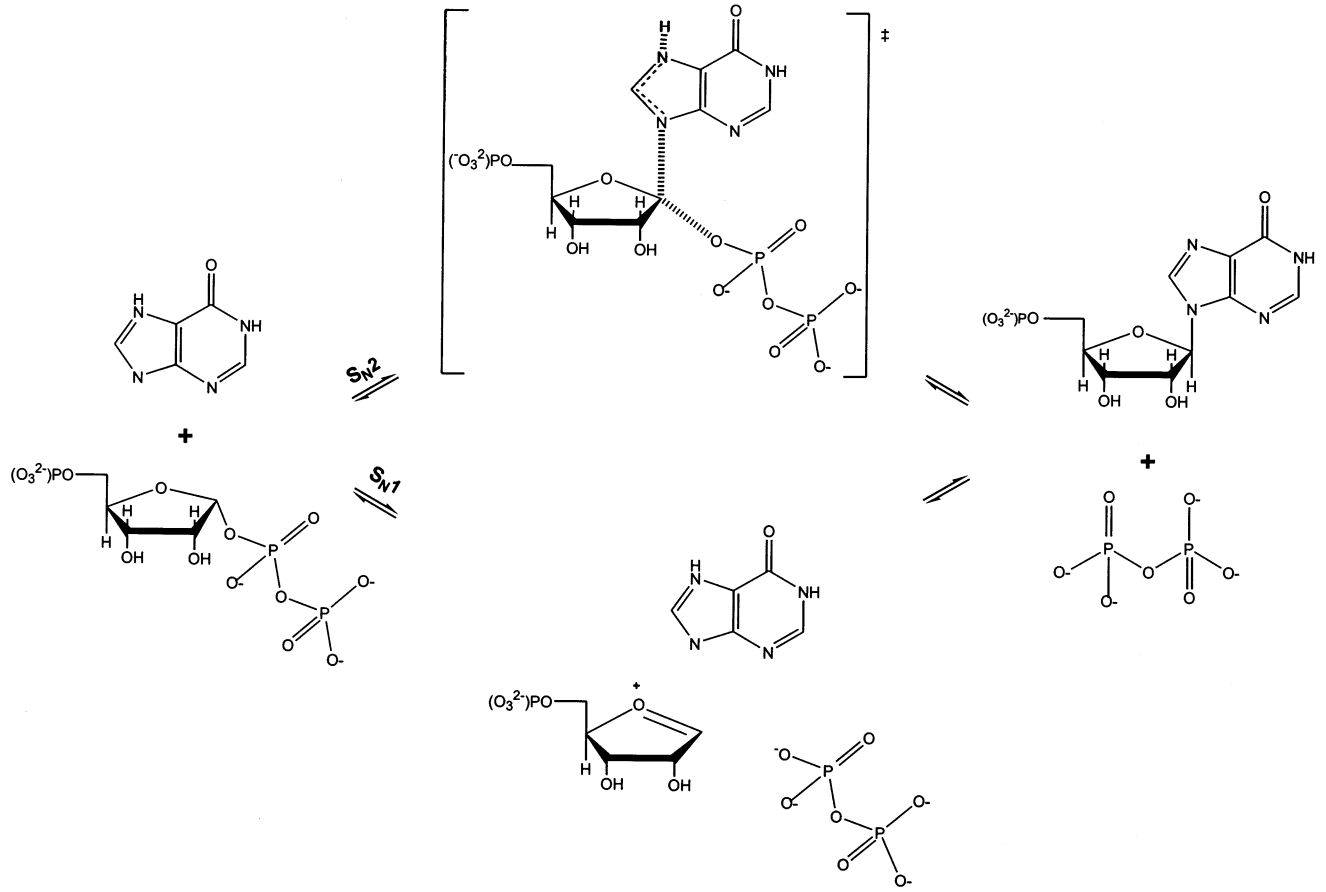

Figure 2. Two possible mechanisms for the reaction catalyzed by the HGXPRTases. Top: an associative (S_N2-like) mechanism. Bottom: a dissociative (S_N1-like) scheme. Most previous work has hypothesized that the hypoxanthine proton departs at the same time or after formation of the sugar−hypoxanthine bond. Our results (see later) suggest that the proton leaves beforehand.

by the purine base and departure of the pyrophosphate occur simultaneously.

Recent experimental evidence on the mechanism of PRTases and other enzymes has been reviewed by Schramm and Shi[6] using a finer definition of reaction mechanisms based on IUPAC nomenclature.[7] They denote the reaction of PRTases as being of type D_NA_N in which the transition state has a partial bond between the purine and sugar but only van der Waals contact between the pyrophosphate and sugar. This was deduced from the analysis of crystal structures of malarial and human PRTases complexed with substrate analogues and transition state inhibitors[2,8−12] and from the results of kinetic isotopic effect (KIE) experiments for the enzymes PNP[13,14] and orotate PRTase.[15,16] In contrast, KIE experiments of the reaction catalyzed by the *N*-ribohydrolase ricin toxin-A chain[17] indicate that this enzyme has a more truly dissociative mechanism, of type D_N *A_N, as there is a cationic ribosyl intermediate with a finite lifetime. A nice summary of the associative or dissociative

(6) Schramm, V. L.; Shi, W. *Curr. Opin. Struct. Biol.* **2001**, *11*, 657−65.
(7) Guthrie, R. D.; Jencks, W. P. *Acc. Chem. Res.* **1989**, *22*, 343−49.
(8) Shi, W.; Li, C. M.; Tyler, P. C.; Furneaux, R. H.; Cahill, S. M.; Girvin, M. E.; Grubmeyer, C.; Schramm, V. L.; Almo, S. C. *Biochemistry* **1999**, *38*, 9872−80.
(9) Shi, W.; Li, C. M.; Tyler, P. C.; Furneaux, R. H.; Grubmeyer, C.; Schramm, V. L.; Almo, S. C. *Nat. Struct. Biol.* **1999**, *6*, 588−93.

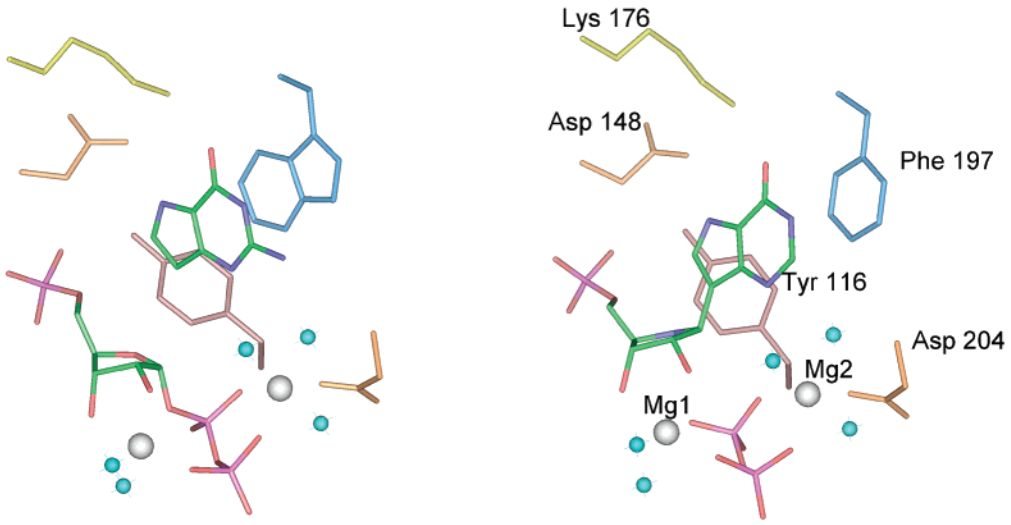

Figure 3. Active sites in the crystal structures of HGXPRTase from *Toxoplasma gondii*[11] (left) and *Plasmodium falciparum*[8] (right). Magnesium ions are in gray, their coordinating water oxygens are in cyan blue, and the phosphate atoms are in purple.

nature of a range of glycosylase reactions, including those mentioned here, has been given recently by Werner and Stivers.[18] Most mechanisms appear to have at least some dissociative character.

In this paper, we present a theoretical study of the mechanism of the malarial HGXPRTase with the hope that any additional light we can throw on the mechanism and its transition state may lead to the design of more efficient inhibitors that could act as antimalarial compounds.[19] The design of mechanistic inhibitors and transition state analogues, such as the immucillins,[20] has already proved to be a promising path to the discovery of antimalarial compounds.[8] The principal tools that we use in our work are free-energy/molecular dynamic simulations in conjunction with a hybrid quantum mechanical (QM)/molecular mechanical (MM) potential. Studies using similar techniques have already been published by us and by others (see, for example, refs 21 and 22 for reviews). To perform such simulations, it is preferable to have available high-resolution crystallographic structures of the enyzme complexed to a ligand that resembles one of the species along the reaction path. Here, we started with the crystal structure of *Plasmodium falciparum* HGXPRTase, complexed with immucillinHP.[8]

The outline of this paper is as follows. Section 2 describes the details of our simulations and the methodological protocols used, section 3 presents the results of our calculations, and section 4 concludes.

2. Computational Details

2.1. Enzyme Model. We took the crystal structure of the enzyme from *Plasmodium falciparum*, refined at a resolution of 2.0 Å,[8] with the protein data bank (PDB)[23] code 1CJB. The structure contains a transition state analogue inhibitor, immucillinHP, pyrophosphate, and two magnesium ions, Mg1 and Mg2. Mg1 is bound to two water molecules, two oxygens of the pyrophosphate and the atoms O2′ and O3′ from the sugar ring, whereas Mg2 is bound to three water molecules, a carboxylic oxygen of Asp 204 and two oxygens from the pyrophosphate. The analogue of the base's aromatic ring lies between the aromatic rings of Tyr 116 and of Phe 197. Figure 3 shows the active site of 1CJB.

For our simulations, we modeled Hx (hypoxanthine) and PRPP from the immucillinHP and pyrophosphate present in the crystal structure. Such an approach is feasible because immucillinHP closely mimics the features expected for ribooxocarbenium ion transition states in malarial and human HG(X)PRTases.[20] Figure 4, in which the ligands in the 1CJB structure and in our starting enzyme model are drawn, illustrates this similarity. Some chemical and geometrical modifications were necessary to do the modeling. The C9 atom was substituted by a nitrogen and the covalent bond between it and the C1′ atom was broken. This was done by translating slightly the base moiety, because the pyrophosphate moiety, with four of its oxygens coordinated to the magnesiums, is more constrained. A bond between the C1′ atom and an oxygen of the pyrophosphate also had to be created to model the PRPP. We did not succeed in finding a stable, docked PRPP structure with the initial coordinations to the metal ion, despite numerous minimization and molecular dynamic calculations. However, while we were engaged in these attempts, a high-resolution crystal structure of the HGXPRTase from *Toxoplasma gondii*, resolved to 1.05 Å, became available (PDB code 1FSG). This structure was the first atomic-resolution structure of a phosphoribosyltransferase containing a PRPP substrate and two magnesium ions.[11] In this structure, whose active site is shown in Figure 3, the oxygen atom bound to the C1′ atom is chelating Mg1. Calculations to model the PRPP from this structure showed better stability and geometric behavior, and the dihedral angles around the atom P1 were less constrained. Therefore, we chose this configuration as our initial one for PRPP.

(10) Focia, P. J.; Craig, S. P., III; Eakin, A. E. *Biochemistry* **1998**, *37*, 17120−27.
(11) Héroux, A.; White, E. L.; Ross, L. J.; Kuzin, A. P.; Borhani, D. W. *Structure* **2000**, *8*, 1309−18.
(12) Balendiran, G. K.; Molina, J. A.; Xu, Y.; Torres-Martinez, J.; Stevens, R.; Focia, P. J.; Eakin, E. A.; Sacchettini, J. C.; Craig, S. P., III. *Protein Sci.* **1999**, *8*, 1203.
(13) Kline, P. C.; Schramm, V. L. *Biochemistry* **1993**, *32*, 13212−19.
(14) Fedorov, A.; Shi, W.; Fedorov, E.; Tyler, P. C.; Furneaux, R. H.; Hanson, J. C.; Gainsford, G. J.; Larese, J. Z.; Schramm, V. L.; Almo, S. C. *Biochemistry* **2001**, *40*, 853−60.
(15) Goiten, R. K.; Chelsky, D.; Parsons, S. M. *J. Biol. Chem.* **1978**, *253*, 2963−71.
(16) Tao, W.; Grubmeyer, C.; Blanchard, J. S. *Biochemistry* **1996**, *35*, 14−21.
(17) Chen, X. Y.; Berti, P. J.; Schramm, V. L. *J. Am. Chem. Soc.* **2000**, *122*, 1609−17.
(18) Werner, R. M.; Stivers, J. T. *Biochemistry* **2000**, *39*, 14054−64.
(19) Craig, S. P., III; Eakin, A. E. *Parasitol. Today* **1997**, *13*, 238−41.
(20) Li, C. M.; Tyler, P. C.; Furneaux, R. H.; Kicska, G.; Xu, Y.; Grubmeyer, C.; Girvin, M. E.; Schramm, V. L. *Nature Struct. Biol.* **1999**, *6*, 582−87.
(21) Amara, P.; Field, M. J. *Computational Molecular Biology*; Leszczynski, J., ed.; Elsevier Science: Amsterdam, 1999; p 1−28.
(22) Gogonea, V.; Suarez, D.; Vaart, A. v.; Merz, K. M., Jr. *Curr. Opin. Struct. Biol.* **2001**, *11*, 217−23.
(23) Bernstein, F. C.; Koetle, T. F.; Williams, G. J. B.; Meyer, E. F.; Brice, M. D.; Rodgers, J. R.; Kennard, O.; Shimanouchi, T.; Tasumi, M. *J. Mol. Biol.* **1977**, *112*, 535−42.

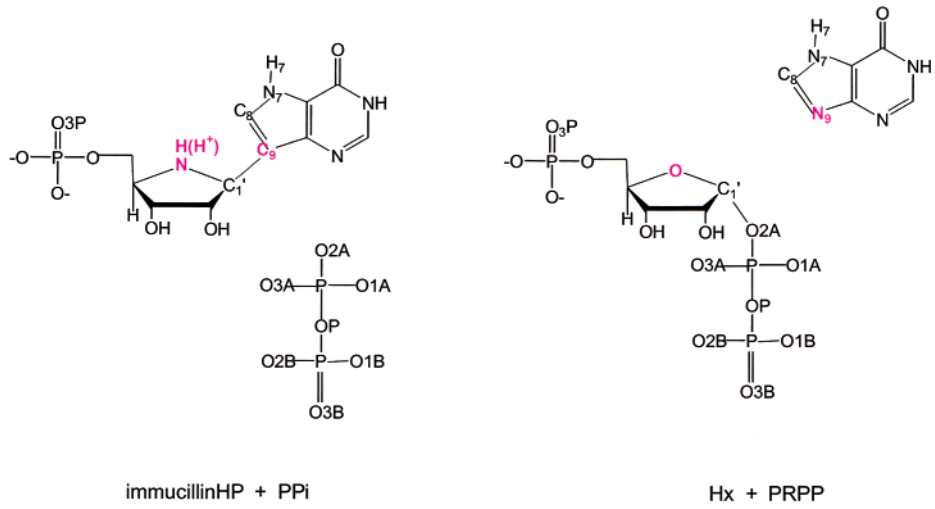

Figure 4. Chemical topologies of the ligands in the *Plasmodium falciparum* HGXPRTase structure (left) and of the natural substrates for the forward enzymatic reaction (right).

Finally, the protonation and tautomerization states of all residues were selected, assuming a pH value of 7. The N7 protonated tautomer of the base was chosen, as this is known to be present prior to catalysis in *N*-ribosyltransferases,[10] even though Hx in solution exists in approximately equal amounts of the N7 and N9 protonated tautomers. The enzyme was solvated as in previous studies[24,25] using a cubic box of water molecules, thermalized at 300 K, with a side of 70 Å. The final system had a minimum of two layers of water molecules around the enzyme and included 129 crystallographic water molecules as well as 6480 water molecules from the water box.

2.2. Hybrid Potential Simulations. All the hybrid potential simulations were done with the DYNAMO program[26,27] using a QM/MM hybrid potential similar to that described in ref 28. For our simulations, the enzymatic system was divided into three concentric zones centered on the reaction site. These consisted of a central QM region, containing the atoms being treated quantum mechanically, a first MM region, in which the atoms were treated with an MM potential and whose atoms were allowed to move in the simulations, and a second MM region, whose atoms were also treated with an MM potential but whose positions were fixed. The AM1 semiempirical method was employed as the QM potential,[29,30] and the all-atom force field of OPLS-AA[31] was used for the MM potential. The AM1 parameters for the magnesium ions were taken from Hutter et al.[32]

A schematic of our partitioning is shown in Figure 5. The three zones are centered on the C1′ atom. For most of our simulations, the QM region contained 75 atoms consisting of the magnesium ions with their coordinating ligands, made up of five water molecules and the side chain of Asp 204, the substrates PRPP and Hx, and the side chain of Asp 148, which has been shown by mutagenesis studies to be the catalytic acid/base. In some of our later simulations, we also included the side chain of Lys 176 in the QM region because this hydrogen bonds to the purine moiety and to Asp 148.[33] This larger model had 83 atoms in the QM region. The inner MM region contained 713 atoms (705 in the larger model) and consisted of all non-QM atoms within a sphere of radius 10 Å centered on the C1′ atom. The remaining atoms in the system were in the outer MM region. The entire simulation system, including protein and solvent, contained 23 533 atoms.

To cope with the covalent bonds between two atoms belonging to the QM and the MM regions, we used the fully automatic link-atom approximation that is implemented in the DYNAMO program and which has been fully explained in ref 27. Link atoms were needed between the Cβ (QM) and Cα (MM) atoms of the residues Asp 204, Asp 148, and, where appropriate, Lys 176.

2.3. Studying the Reaction Mechanism. The reaction mechanism of the enzyme was investigated using three different types of simulation technique: (1) hybrid potential calculations with the AM1 semiempirical QM method to calculate the free-energy surface for the reaction, (2) reaction-path calculations with both semiempirical and ab initio hybrid potentials, and (3) saddle-point location and normal-mode analyses with the QM(AM1)/MM hybrid potential.

The procedures for the free-energy (1) and reaction-path calculations (2) were almost exactly the same as those that we have detailed in our previous publications (see, for example, refs 24 and 25) and so will not be repeated here. The only difference was in the quantum chemical density functional theory (DFT) calculations for which we used a 6-31++G** basis set.[34] The saddle-point calculations were performed as follows:

1. Structures corresponding to reactant and product minima and to the transition state were selected from the minimized pathways determined with the semiempirical hybrid potential (type 2 in the previous list).

2. These structures were refined using the standard eigenvector-following geometry-optimization procedure implemented in the DYNAMO program.[26] To reduce the cost of these calculations (principally due to the calculation of the second derivatives), the positions of all atoms were fixed except for those directly implicated in the reaction (about 75 in total).

3. Once the saddle point had been characterized, it was verified to lead to the correct minima by visual inspection of the displacements produced by the normal mode of imaginary frequency and by generating the intrinsic reaction coordinate using a finite-difference procedure.

(24) Thomas, A.; Jourand, D.; Bret, C.; Amara, P.; Field, M. J. *J. Am. Chem. Soc.* **1999**, *121*, 9693−702.
(25) Proust-De Martin, F.; Dumas, R.; Field, M. J. *J. Am. Chem. Soc.* **2000**, *122*, 7688−97.
(26) Field, M. J. *A Practical Introduction to the Simulation of Molecular Systems*; Cambridge University Press: Cambridge, U.K., 1999.
(27) Field, M. J.; Albe, M.; Bret, C.; Proust-De Martin, F.; Thomas, A. *J. Comput. Chem.* **2000**, *21*, 1088−100.
(28) Field, M. J.; Bash, P. A.; Karplus, M. *J. Comput. Chem.* **1990**, *11*, 700−33.
(29) Dewar, M. J. S.; Zoebisch, E. G.; Healy, E. F.; Stewart, J. J. P. *J. Am. Chem. Soc.* **1985**, *107*, 3902−09.
(30) Dewar, M. J. S.; Dieter, K. M. *J. Am. Chem. Soc.* **1986**, *108*, 8075−86.
(31) Jorgensen, W. L.; Maxwell, D. S.; Tirado-Rives, J. *J. Am. Chem. Soc.* **1996**, *118*, 11225−36.
(32) Hutter, M. C.; Hughes, J. M.; Reimers, J. R.; Hush, N. S. *J. Phys. Chem. B* **1999**, *103*, 4906−15.
(33) Xu, Y.; Grubmeyer, C. *Biochemistry* **1998**, *37*, 4114−24.
(34) Koch, W.; Holthausen, M. C. *A Chemist's Guide to Density Functional Theory*. Wiley-VCH: Weinheim, Germany, 1999.

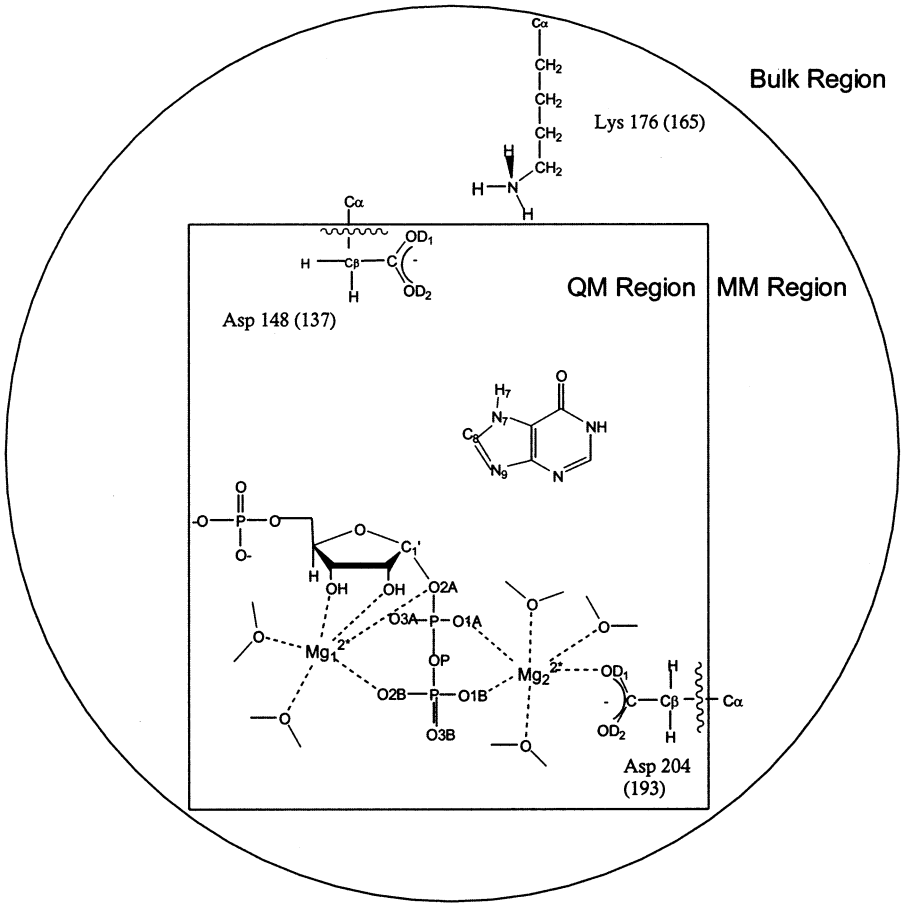

Figure 5. Partitioning into QM, MM, and Bulk Regions for the QM/MM simulations. The QM region represented in this figure contains 75 atoms.

4. Finally, normal-mode analyses were performed at all the characterized stationary points.

3. Results

The results of the three different types of simulation will be discussed in turn.

3.1 Free-Energy Calculations. As in our previous studies,[24,25] we calculated free-energy curves and surfaces for the enzyme mechanism as functions of geometrical variables which we considered could describe sufficiently well the reaction. The choice of variables necessitated some trial and error, but we shall not detail all our attempts here. In the end, however, we found that the best description of the reaction could be obtained in terms of two composite variables, both of which involved the difference of two distances. The variables were $RC1 = d(\mathrm{N9-C1'}) - d(\mathrm{C1'-O2A})$ and $RC2 = d(\mathrm{H7-N7}) - d(\mathrm{OD1(Asp148)-H7})$. $RC1$ permits the description of the reaction bond-breaking and forming processes about the C1′ atom of the sugar, whereas $RC2$ allows proton transfer between the purine and the side chain of Asp 148. It was essential to include both variables, as the two processes of proton transfer and of ribose transfer were found to be intimately linked. An initial trial in which the distances d(N9−C1′) and d(C1′−O2A) were treated separately did not produce significantly different results.

The free-energy surface obtained from the calculations with $RC1$ and $RC2$ is shown in Figure 6. The calculation of the surface required 1225 simulations, each of 10 ps. The preferred pathway, marked in white on the figure, proceeds via two steps. The first step, which has a barrier of about 30 kJ mol^{-1}, is a deprotonation of Hx by the side chain of Asp 148 to form an intermediate (marked INT). The second step involves the formation of the bond between the ribose and the base moiety and departure of PPi; it is rate determining with a barrier of around 90 kJ mol^{-1}. This should be compared to the experi-

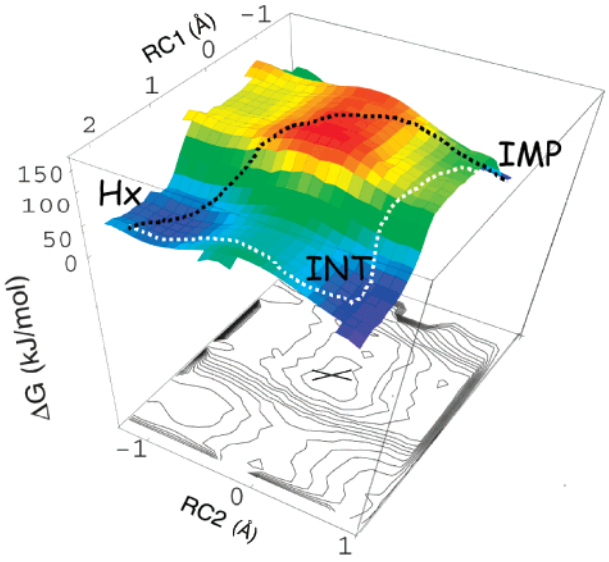

Figure 6. Calculated free-energy surface for the reaction in terms of the two variables $RC1$ and $RC2$. The path in black dots represents the direct path for the conversion of Hx into IMP. The white dotted path is the alternate path, going via the metastable structure INT. Also shown is the two-dimensional contour map projection of the surface with contours at 10 kJ mol^{-1} intervals.

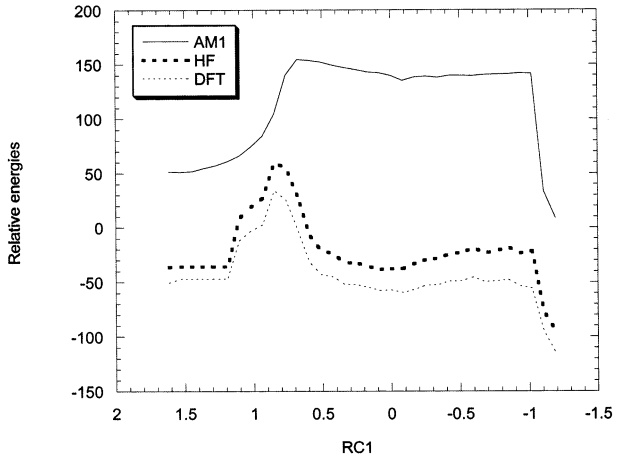

Figure 7. QM AM1, Hartree−Fock, and DFT energies of structures along the minimized pathway for the ribose-transfer step of the stepwise reaction mechanism shown in Figure 6. As only the relative energies between structures within each path are meaningful, the curves have been displaced with respect to one another for clarity.

mental value for the catalysis of Hx in human HGPRTase which has been kinetically estimated to be about 63 kJ mol^{-1}.[5] There is a direct pathway, marked in black dots on the surface, that involves concerted proton and ribose transfer, but this has a much higher energy (∼150 kJ mol^{-1}). The reactants, products, and intermediate structures are approximately isoenergetic.

We also tried a series of calculations with Lys 176 added to the QM region because we wanted to check whether this residue, whose side chain hydrogen bonds to the side chain of Asp 148, could partake in the reaction. We found very little difference, however, in the results between the two different models, in agreement with mutagenesis studies[33] that show that Lys 176 is critical for binding of the purine moiety but is not involved in the catalysis.

3.2. Reaction-Path Calculations. To verify the results of the free-energy calculations obtained with the semiempirical method, we computed minimum-energy reaction paths with both semiempirical and ab initio hybrid potentials for the stepwise mechanism that is predicted to be the most favorable. Perhaps somewhat surprisingly, when given the known inadequacies of the AM1 method in this regard, the semiempirical and ab initio results agree well for the proton-transfer step (data not shown). The results for the second step showed more discrepancy and are illustrated in Figure 7. Although the AM1 profile shows a much broader plateau, the profiles display the same qualitative character. The points of highest energy occur at equivalent values of the reaction coordinate, and the energy barriers are similar although the ab initio barriers are slightly smaller (∼80 compared to ∼100 kJ mol^{-1}).

3.2.1. Transition State Analysis. To further characterize the ribose-transfer step of the stepwise reaction mechanism, we located the saddle point along the minimized reaction path obtained with the semiempirical hybrid potential. The structure has C1′−N9 and C1′−O2A distances of 2.56 and 1.80 Å, which corresponds, in the definitions listed by Schramm and Shi,[6] to a D_NA_N mechanism, as the leaving pyrophosphate is still relatively closely bound and the nucleophile is at a longer distance.

Experimentally, transition state structures have been proposed for two other *N*-ribosyl transferases, PNP[13] and orotate PRTase.[16] In the first case, the distances C1′−N9 and C1′−O2A are equal to 1.77 and 3.01 Å, respectively, whereas in the second they are 1.85 and 3.80 Å. These values are roughly inverse to the ones we obtain for the malarial HGXPRTase, but it may be that direct comparisons are difficult because the conditions of study were not the same. Aside from the fact that the enzymes are different, the experiments used non-natural ligands, such as arsenate and phosphonoacetic acid, as replacements for the attacking PPi nucleophile.

The structure of the saddle point along the path leading from INT to IMP had a single imaginary frequency with a value of 393*i* cm^{-1}. The motion induced by the imaginary mode is preponderantly that of the C1′ atom with minor movements, in decreasing order, of O2A, C2′, O (in P−O−P), and C3′. Analysis of the motions generated during the free-energy calculations confirm these results and also agree with those predicted for the reaction path derived from an analysis of the crystal structure[8] and in which the primary reaction coordinate motion is the movement of the ribosyl C1′ between the relatively immobile purine base and the Mg2-bound pyrophosphate.

As stated above, the principal movement in the ribose-transfer step occurs for the C1′ atom. In general, the geometry of the remaining atoms changes little, although we would like to emphasize the following points:

- The sugar ring pucker is C3′ endo in free nucleotides, but its configuration is C2′ endo C3′ exo in the starting crystal structure and remains so throughout the simulations.
- The distances between the magnesiums and their chelating oxygens vary between 2.0 and 2.3 Å. They change little throughout the reaction.
- The geometry of the pyrophosphate moiety remains similar throughout the path except that the valence angle around the central oxygen increases from a value of 139° in PRPP to 156° roughly halfway along the path leading from INT to IMP.
- The PRTases possess a conserved aromatic residue that provides a $\pi-\pi$ stacking interaction with the purine substrate. In the malarial HGXPRTase, this role is played by Tyr 116. Its orientation and position with respect to the purine remains stable throughout the simulations, and there is a stable hydrogen bond with a distance of ∼2.8 Å between the tyrosine hydroxyl group and O3P.
- In addition to the transition state structure, it is interesting to look at how the geometry of the system changes at other points along the reaction path. Figure 8 shows plots of some interatomic distances as a function of the reaction coordinate, *RC*1, gleaned from the free-energy simulations. The transition state on the minimum energy path occurs at an *RC*1 value of about 0.8 Å. It can be seen that, throughout most of the path, the ribose is bonded to neither Hx nor PPi because the C1′−O2A bond breaks at RC1 ≈ 1 Å and the C1′−N9 bond does not form until *RC*1 ≈ −1 Å.

In addition to the stepwise pathway, it also proved possible to characterize a saddle-point structure for the concerted mechanism (the black cross in Figure 6), although it was higher in energy by 50 kJ mol^{-1}. The single imaginary frequency had a value of 1193*i* cm^{-1}, and the distances between the reacting atoms were as follows: C1′−N9, 2.55 Å; C1′−O2A, 2.54 Å; H7−N7, 1.27 Å; and OD1(Asp148)−H7, 1.23 Å. This structure resembles the transition state of a reaction with an A_ND_N mechanism (corresponding to a concerted S_N2-like displace-

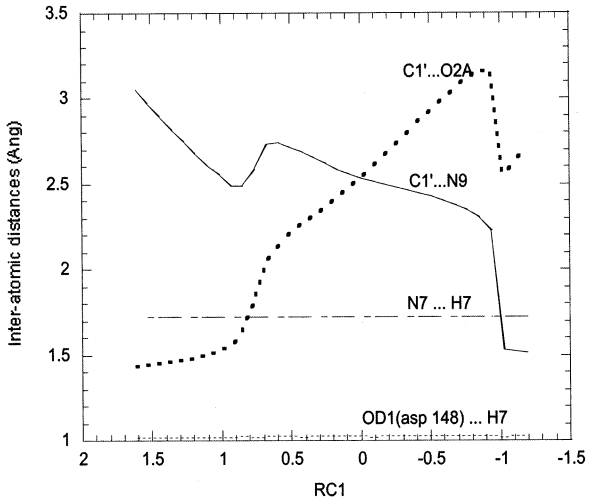

Figure 8. Plot of some interatomic distances as a function of the reaction coordinate *RC*1 for the ribose-transfer step of the stepwise reaction mechanism. The distances are calculated as means of those found during the MD simulations for each value of *RC*1. The maximum standard deviations of these distances about their means are 0.15 Å for C1′−O2A and C1′−N9 and 0.05 Å for N7−H7 and OD1−H7.

ment[7]), although the two partial bonds, C1′−N9 and C1′−O2A, are perhaps a little too long for the mechanism to be truly considered A_ND_N.[6] It is worth remarking that the distance between the atoms OD1 and N7 at this transition state is short (∼2.5 Å), and a similar distance is observed at the top of the barrier for the proton-transfer step in the stepwise pathway. These distances are reminiscent of those found for low-barrier hydrogen bonds, which have been postulated to be important in enzyme catalysis.[35]

4. Discussion

In this paper, we have presented a study of the reaction mechanism of the malarial HGXPRTase, which converts Hx and PRPP into IMP and pyrophosphate. The calculations were performed with the DYNAMO program using semiempirical and ab initio hybrid potentials[26,27] and a mixture of free-energy, reaction-path, and saddle-point location calculations. The preferred pathway is predicted to be stepwise with a rapid proton transfer between the N7 atom of Hx and the side chain of Asp 148 followed by the rate-limiting ribose transfer. The calculated energy barrier is in reasonable agreement with that observed experimentally. The mechanism can be classified, following IUPAC nomenclature,[7] as being of type D_NA_N because the transition state for the ribose-transfer step of the reaction has a structure in which the breaking sugar−PPi bond is short (∼1.8 Å) compared to the distance between the attacking nucleophile and the sugar (∼2.6 Å). This mechanism is partially dissociative, as the breakage of the C1′−O2A bond occurs before the formation of the C1′−N9 bond. Our studies agree with mutagenesis results which show that Asp 148, but not Lys 176, is catalytically active.

Many other glycosylases have been shown to have mechanisms of dissociative character (see ref 18 for a review), and transition states typical of D_NA_N-type mechanisms have been deduced experimentally for two other *N*-ribosyl transferases, namely PNP and orotate PRTase (see ref 6 for a review). The structure of our transition state differs, though, from those proposed by these workers for reasons discussed in section 3.2.1. Another aspect of our results deserving discussion concerns the fact that, in our mechanism, the transition state involves a hypoxanthine anion because the proton transfer between Hx and the protein is rapid and occurs separately. The majority of previously proposed mechanisms have postulated that the N7 atom is protonated in the transition state and so proton transfer occurs either simultaneously with or after glycosyl transfer. Experimental support for a N7-protonated transition state has come from KIE measurements of a nucleoside hydrolase[36] and the ricin toxin-A chain[17] reactions.

To help resolve some of the questions raised by the present study, we are continuing our work on the reaction mechanism of this enzyme using more sophisticated reaction-path-finding and ab initio hybrid potentials. We are also studying the mechanism of the human version of the enzyme, HGPRTase, which has a 44% sequence identity with the parasitic enzyme and does not use xanthine as a substrate, differences that may be enough to propose specific inhibitors to the parasitic enzyme. The results of these calculations will be presented in due course.

Acknowledgment. The authors would like to thank the referees of this paper for helpful comments, Flavien Proust and Vern Schramm for stimulating discussions at various stages of this work, the staff at the computer center of the CEA in Grenoble for technical assistance, and the Institut de Biologie Structurale Jean-Pierre Ebel (CEA/CNRS) for financial support.

JA0206846

(35) Cleland, W. W.; Frey, P. A.; Gerlt, J. A. *J. Biol. Chem.* **1998**, *273*, 25529−32.

(36) Horenstein, B. A.; Parkin, D. W.; Estupiñán, B.; Schramm, V. L. *Biochemistry* **1991**, *30*, 10788−95.